

Empirical Study on the Effect of Tungsten Carbide Grain Size on Wear Resistance, Cutting Temperature, Cutting Forces and Surface Finish in the Milling Process of 316L Stainless Steel

Emilia Franczyk^{1*}, Marcin Małek¹

¹ Cracow University of Technology, Mechanical Faculty, al. Jana Pawła II 37, 31-864, Krakow, Poland

* Corresponding author's e-mail: emilia.francyk@pk.edu.pl

ABSTRACT

Cutting tools made of the WC-Co sintered carbides are now very popular and are widely used in machining of materials. However, there are numerous problems in this area which require more research and need to be studied further. This paper presents the results of an experimental study aimed at discovering the impact of the microstructure, particularly of the tool substrate grain size, on the quality of the machined surface, cutting forces and temperature in the cutting zone, as well as the tool life. In addition, the impact of the feed was considered. The machining process involved side milling of a cuboidal block made of the AISI 316L steel which, due to its specific properties, is widely used in many industries. The tools used in the tests had different WC phase grain size: 0.18, 0.28 and 0.31 μm , respectively, and moreover the middle specimen had also a non-homogeneous structure and an increased content of the Co matrix. The tests proved a significant impact of the tool microstructure on the tool life and the roughness parameters R_a and R_z of the machined surface. The impact of the studied factors on the forces and the temperature in the cutting zone was not as strong, because it did not exceed 20%. The value and the novel character of the paper results from the fact that it concerns a specific case: side milling of the 316L steel with the use of the WC-Co sintered carbide tools, and consequently provides a contribution to solve a practical industrial issue.

Keywords: 316L stainless steel, sintered carbide grain size, wear, cutting temperature, cutting forces, surface roughness

INTRODUCTION

Due to their durability, resistance to corrosion and oxidation at high temperatures and very good hygienic properties, austenitic stainless steels are widely used in many areas of technology. For this reason they account for 70% of worldwide market share of all stainless steels [1]. The 316L steel, which is the subject of this study, belongs to 300 series grades of austenitic stainless steels which contain 16–26% of chromium and 6–22% of nickel. The letter “L” in the grade designation indicates a low carbon content (about 0.03%), resulting in a good weldability and exceptional resistance to corrosion [1, 2]. Unfortunately, the machining of stainless steels is a complex and difficult process, the reason being, among other

things, their low thermal conductivity and high ductility [1, 3]. Song et al. [4] emphasize that the 316L steel has a tendency to work-hardening during deformation and has a high susceptibility to deformation-induced martensitic transformation. The attempts to increase the machining parameters – cutting speed, feed and depth of cut – cause a significant increase of cutting forces and lead to defects resulting from residual stress [5]. Fernández-Abia et al. [2] also indicate that poor machinability of austenitic steels results from their relatively high friction coefficient at the material–tool interface, high thermal dilation which makes it difficult to maintain machining tolerances and a large area of ductile strain causing very long chips and a built-up edge (BUE) on the cutting tool. Difficult cutting conditions lead to increased

costs and process emissivity which negatively affects the process general sustainability and creates the need for its optimization [6–8].

Wear of cutting tools is an important problem during the machining of stainless steels. The type of wear depends on the values of feed and cutting speed, and consequently on the cutting forces and temperatures [9]. Large surface pressures and increased temperatures (e.g. at high cutting speeds) cause the increased adhesion wear manifesting itself in formation of built-up edge [10, 11]. According to many authors, in addition to abrasive and diffusion wear, the adhesion wear is especially critical in the case of machining of stainless steels as it may lead to the crater wear, flank wear, chipping and finally to failure of the tool [12–14]. It should be noted that the tool wear can affect other output parameters of the cutting process. Martinho et al. [15] concluded that a uniform wear of the cutting tool is necessary for a good surface finish.

In connection with the difficulties mentioned above, actions are taken both in industry and science in order to improve the quality and effectiveness of machining of stainless steels. One common way in this context is an attempt to improve the knowledge and control of the machining environment and parameters. Many authors presented the impact of parameters such as cutting speed, feed, depth of cut on the machined surface roughness, cutting force and tool wear [16–18]. Leppert as well as Das and Ghosh [19] showed the influence of the cutting zone cooling and lubrication on the cutting force as well as on surface roughness and its defects. Szczotkarz et al. [20] by using Minimum Quantity Lubrication (MQL) obtained a significant reduction of the adhesion wear. Natesch et al. [21] proved that the type of lubricating medium also affects the main process outputs.

A parallel line in the development comprises attempts to optimize the design of cutting tools by using new coatings or tool materials. According to Inspector and Salvador [22] over 90% of all cemented carbide tools are currently coated with protective layers. AlTiN and AlCrN-based coatings are commonly used for carbide tools intended for machining of stainless steels due their high hot hardness and oxidation resistance [23]. The problem of tool coatings and their effectiveness in the area of machining of difficult-to-cut materials has been raised by numerous authors and is generally well researched. The results of studies on

this matter were presented, inter alia, by Kulkarni et al., Ciftsi, Endrino et al. [11, 23, 24]. In terms of tool coatings, the studies are conducted also on the impact of grain size of the coating on the cutting performance of the tools, and the results of such studies have been presented by, inter alia, Bouzakis et al. and Tillmann et al. [25, 26].

Equally important as the studies on the coatings are studies on the tool substrate structure. In general, cemented carbide consists of WC hard phase and Co binder phase [27]. It is known that hardness and toughness of cemented carbides depend on WC grain size and Co content [28, 29]. In their work, Bouzakis et al. [30] showed that the finer the grains, the higher the tool substrate hardness, and the coating deposited on such substrate has a better mechanical strength than in remaining cases. At the same time, they showed a good adhesion of the coatings on all the examined substrate grain sizes. Tang et al. [31] investigated the relationship between the WC grain size, microstructure and properties of the substrate and coatings. They found that the microhardness was similar in all tested and that the increase of the grain size in the substrate improves bonding strength of the coating. Jian et al. [32] also found a significant impact of the substrate grain size on the performance of diamond films deposited on tungsten carbide cutting tools. Polini et al. [33] showed a major role of substrate grain size in determining the cutting performance of diamond coated WC-Co tools; however they referred only to the tool wear, and their workpiece was aluminum-based. It is worth mentioning that the microstructure and therefore mechanical properties of sintered tools can be modified by changing the parameters of the sintering process. For example, Parihar et al. [34] found that the improvement in mechanical properties (hardness, fracture toughness) of WC-Co sinters can be obtained by increasing sintering temperature and heating rate.

The literature review above indicates that the knowledge of the impact of the structure of cemented carbides on the properties of tools and objects manufactured in the machining process with the use of such tools needs to be expanded. To the best knowledge of the authors, the studies on the direct impact of the tool substrate grain size on the outputs of the machining process of austenitic stainless steels have not been published to date. Thus, the research presented in this paper is novel.

MATERIALS AND METHODS

This section describes the test stand setup, the machining process used and equipment and measurement methods applied in the studies. The last subsection presents the detailed plan of the experiment.

Work material

In the present work, the AISI 316L austenitic stainless steel has been selected as a work material due to its wide applications in many industries and its poor machinability. The specimens used were 100×100×50 mm blocks. The basic mechanical properties of the steel and chemical composition are presented in Tables 1 and 2, respectively [21].

Milling tools

The tools used in the tests were carbide end mills of diameter 12.0 mm, working part length of 26.3 mm and total length of 83.0 mm. The geometrical details are presented in Figure 1. The milling cutters were made with the use of the 5-axis grinding method from WC-Co sintered carbide solid bars of various grades: MK12, JF15 and GA20. Before applying protective coatings in PVD processes, all tools were subject to an additional technological procedure in the form of rounding the cutting edge in order to improve the durability of the tools. For each tested prototype, the drag finish process was performed in identical conditions in order to obtain a similar value

of rounding of the main cutting edge. In order to verify this value after the production process, each prototype was measured using an Alicona Infinite Fokus microscope. The photographs of the microstructure of each sample presented in Figure 2 were taken with the scanning electron microscope FEI Quanta 3D FEGSEM integrated

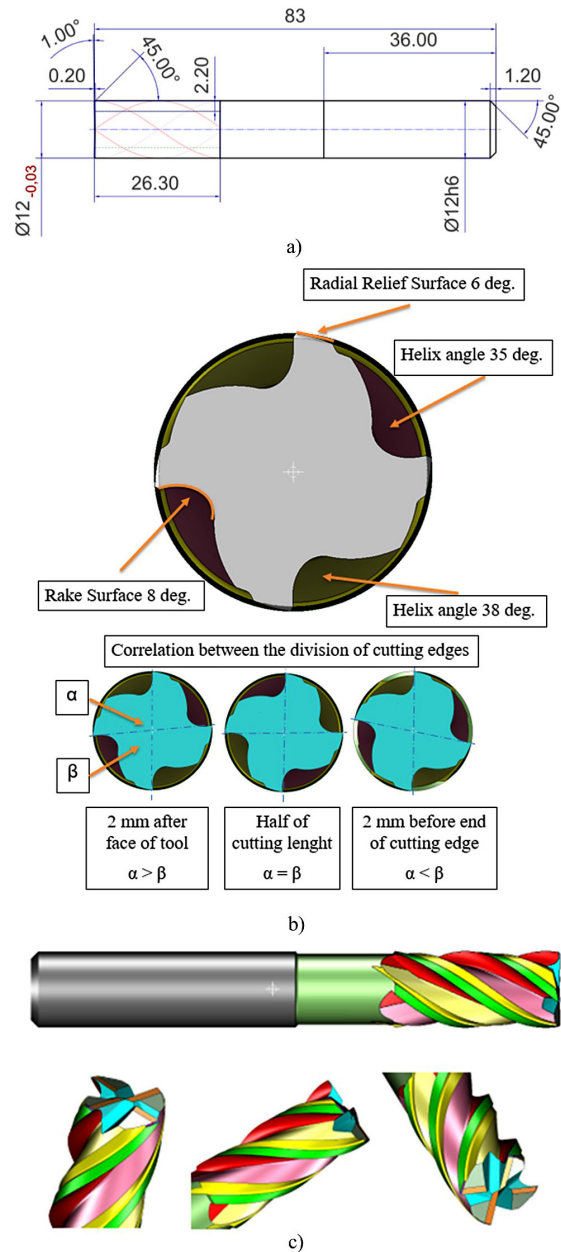


Figure 1. Technical drawing of the milling cutters used in the tests. (a), geometric parameters of the milling cutters used in the tests (b), visualisation of the designed milling cutter (c)

Table 1. General mechanical properties is of the AISI 316 L

Specification	Typical value
Hardness, Rockwell B	95
Ultimate tensile strength (MPa)	485
Yield tensile strength (MPa)	170
Modulus of elasticity (GPa)	200
Poisson's ratio	0.3
Density (g/cm ³)	7.9
Elongation (%)	40
Fatigue strength (MPa)	146

Table 2. Chemical composition (%) of AISI 316L stainless steel

Element	C	Mn	Si	P	S	Cr	Mo	Ni	N
Wt (%)	0.03	2.00	0.75	0.05	0.03	18.00	3.00	14.00	0.10

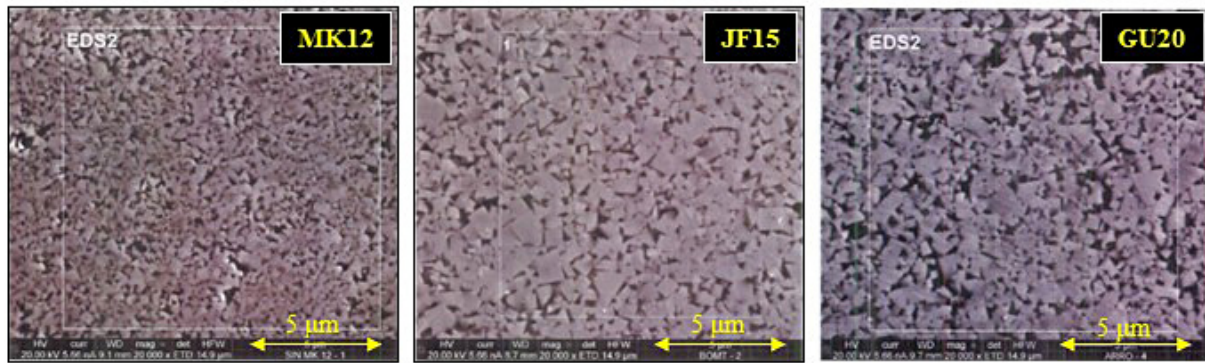


Figure 2. Microstructure of tested tools

with the EDAX Trident analysis system. The chemical composition analysis was performed based on the X-ray energy dispersive spectroscopy, using the ZAF correction procedure. The cemented carbide grain size was determined with the use of the Feret method. The proposed tool solution is a prototype created for the needs of machining austenitic steels. As shown by Table 3, the basic parameter that differentiated the carbides was the grain size. The GU20 sample had also a more non-homogeneous structure and an increased content of the Co matrix.

All tools were covered with the AlCrN-based coating BALINIT® ALNOVA made by Oerlikon Balzers Coating AG by means of cathodic arc deposition (Arc-PVD, where PVD means physical vapour deposition). This kind of coating is recommended for machining of stainless steels [23].

Milling process

The machining process involved a side milling of a 316L steel block according to the diagram presented in Figure 3. The successive steps of the experiment (n) involved the removal of a material layer of a width $a_p = 20$ mm and depth $a_e = 1$ mm at a constant cutting speed $v_c = 80$ m/min. The feed per tooth was a variable parameter whose values were in the range $f_z = \{0.04; 0.06; 0.08\}$ mm/tooth, where z is the number of teeth in the tool.

Test stand, measurement methods

The core of the test stand presented in Figure 4 was the vertical HAAS MiniMill 2 vertical milling centre (1) used to perform the machining process.

Table 3. Physical parameters of tested carbides (manufacturer’s data)

Grade	Grain size (μm)	Cobalt content (wt%)	Hardness HRA
MK12	0.18	9.5	92.5
JF15	0.31	9.7	92.3
GU20	0.28	10.4	92.0

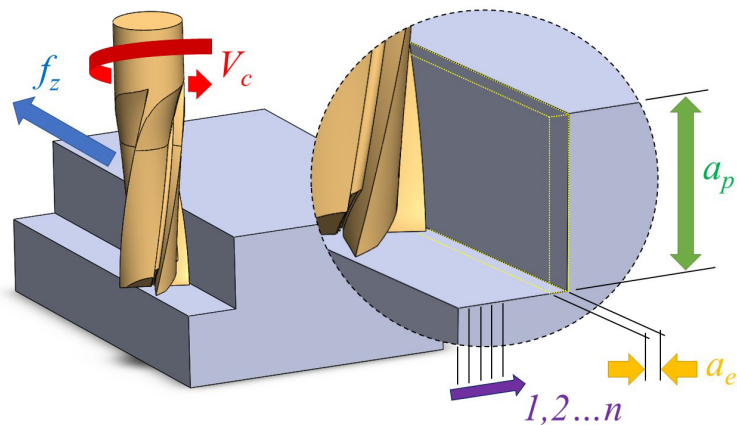


Figure 3. Milling process scheme

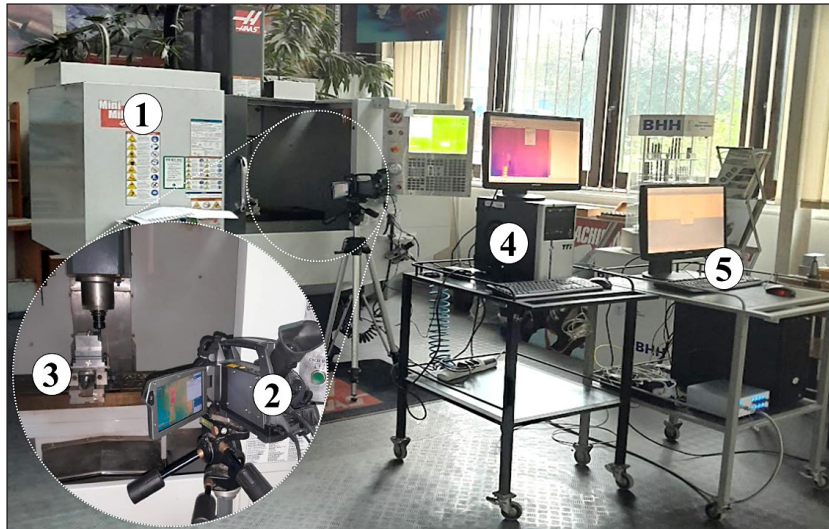


Figure 4. S Test stand (1) –HAAS MiniMill 2 milling machine, (2) – thermovision camera, (3) – dynamometer, (4) –PC with camera operation software, (5) PC with dynamometer operation software

The test stand was equipped with the FLIR SC620 (2) thermovision camera used to record the temperature in the cutting zone. The 640 x 480 px images were recorded at the 30 fps sampling frequency, and the used emissivity factor was $\epsilon = 0.6$ [35]. A PC (3) with ThermaCam Researcher 2.9 software was used to collect and analyse the measurement data. Figure 5 shows an example of an image obtained. The maximum value of temperature obtained during a given test was used in the analysis of data. The maximum value of temperature obtained during a given test was used in the analysis of data. During the tests, the maximum temperature in the cutting zone was

measured (measurement area is marked with a blue rectangle in Figure 5). The temperature value was recorded on a graph as a function of time.

The cutting forces were measured using a Kistler 9257B piezoelectric dynamometer (3) mounted on the milling machine tool table. The measurement setup included a Kistler 5070B charge amplifier, and the measurement results were recorded at 1 kHz frequency on the PC (5) with DynoWare v.2825A software also provided by Kistler. The cutting forces were measured in three perpendicular directions, however for the preparation of results the forces measured in the plane perpendicular to the milling cutter axis were used, i.e. forces F_x and F_y .

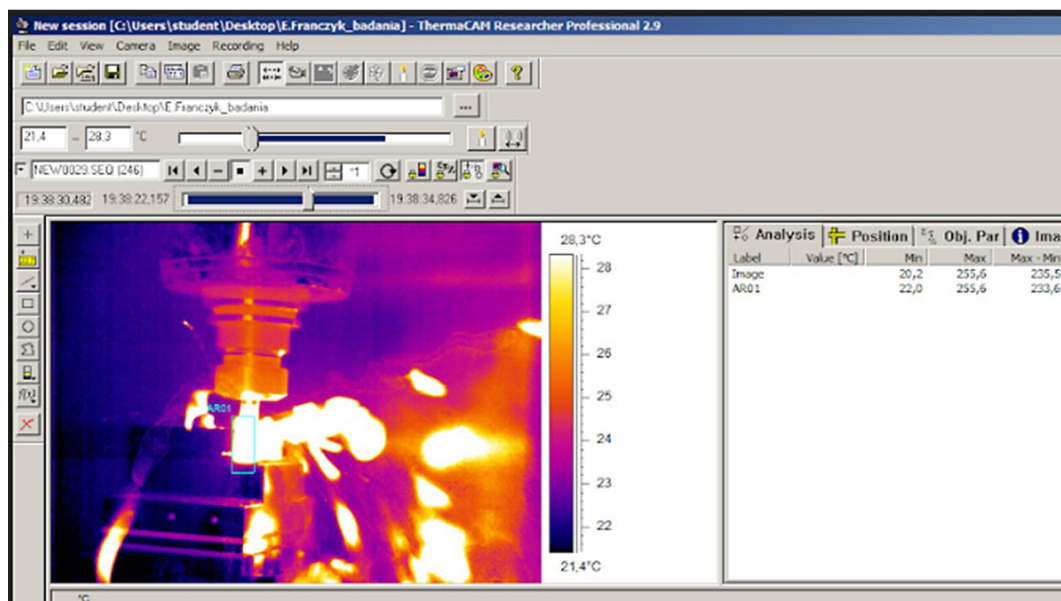


Figure 5. Example of image obtained by means of thermovision camera

The surface finish was evaluated using a Mahr MarSurf PS10 roughness measuring instrument equipped with an inductive sliding head with the 2 μm tip radius and the contact force of approximately 0.7 mN. The instrument allows a profilometric measurement of a section at 8 nm resolution and in the range up to 350 μm. In each test, Ra and Rz parameters were measured in three equally placed zones over a measurement length of 4.8 mm, where the physical measurement length was 4 mm, as shown in Figure 6, and the result of each test was their arithmetic mean.

The tool wear was measured with the use of a DinoLight microscope in combination with a Zoller Genius measuring instrument. The parameter used to evaluate the tool wear was the tool flank wear width VB (mm) which is generally used to estimate the cutting capabilities of a tool [36, 37]. VB measurement was achieved using Zoller genius

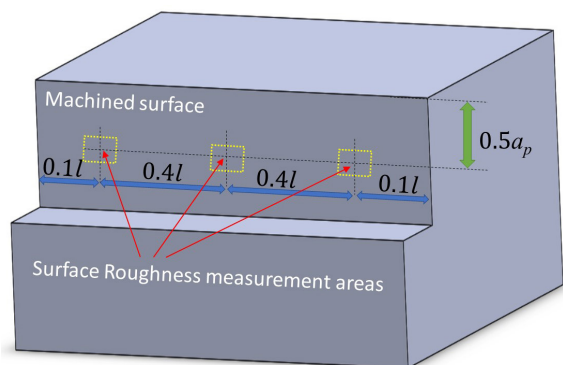


Figure 6. Method and surface roughness measurement areas

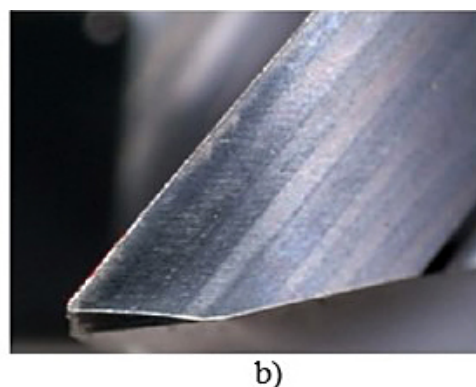
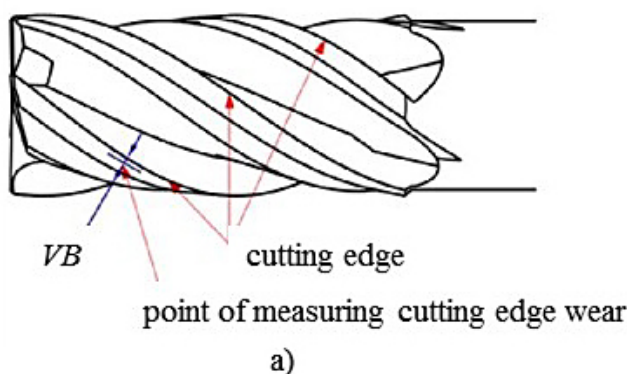


Figure 7. Determination of VB (a) and cutting edge photograph (b)

machine and Dino Light USB microscope. The method of VB determination and an example of microscope photograph are presented in Figure 7.

Experiment design

The tests were divided into two principal parts. The first part of the experiment involved the determination of the impact of the tool grade on the machined surface finish (Ra, Rz), cutting forces F_x and F_y and the maximum temperature in the cutting zone T_{max} . The tests were conducted for three different feed values, and each test was repeated three times, each time with a new tool to eliminate the impact of the tool wear on the obtained results. In total, 27 tests were conducted as shown in Table 4.

The second part of the experiment involved the impact of the tool substrate grain size and microstructure on the tool wear. The constant feed $f_z = 0.06$ mm/tooth was used. The condition of the edge was checked every 3 minutes and the milling process was continued until for a given case the VB reached 0,2 mm ($t_{VB0.2}$).

RESULTS AND DISCUSSION

Surface finish, cutting forces and cutting temperature

The results obtained in the first part of the studies are presented in Figures 8 to 10. Figure 8 shows the measured surface roughness parameters

Table 4. Plan of the first part of the experiment

Test No.	1÷3	4÷6	7÷9	10÷12	13÷15	16÷18	19÷21	22÷24	25÷27
Feed f_z (mm/z)	0.04	0.06	0.08	0.04	0.06	0.08	0.04	0.06	0.08
Grain size (μm)	0.18	0.18	0.18	0.28	0.28	0.28	0.31	0.31	0.31

R_a i R_z , Figure 9 describes cutting forces F_x i F_y , and the maximum temperatures obtained (T_{max}) are presented in Figure 10. In each case, the variables on the horizontal axis are carbide (tool) grade and feed per tooth. The dots on the graphs represent the mean value from three trials, and whiskers represent the standard deviations.

The microstructure analysis of used carbides and the results obtained in this part of the experiment leads to the conclusion that the studied parameters are affected not only by the grain size but also by the content of the WC component in the carbide.

The lowest temperatures in the cutting zone were obtained for the carbide with 0.31 μm grain

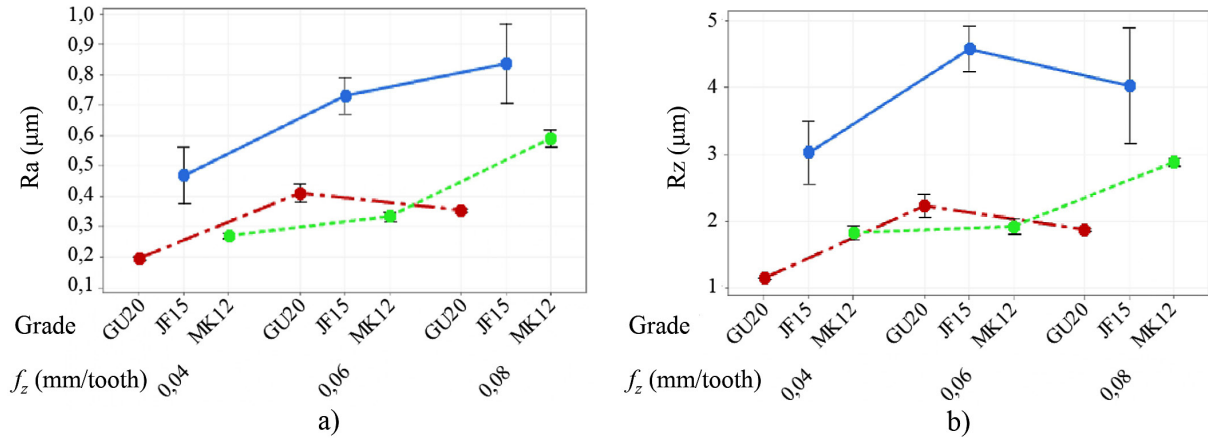


Figure 8. Surface roughness R_a (a) and R_z (b) vs. tool grade and feed f_z

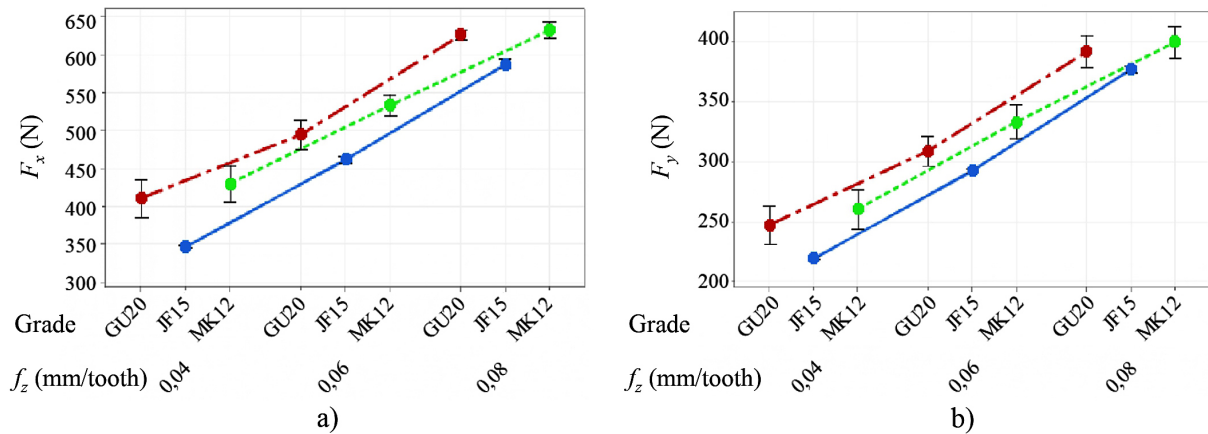


Figure 9. Cutting forces F_x (a) and F_y (b) vs. tool grade and feed f_z

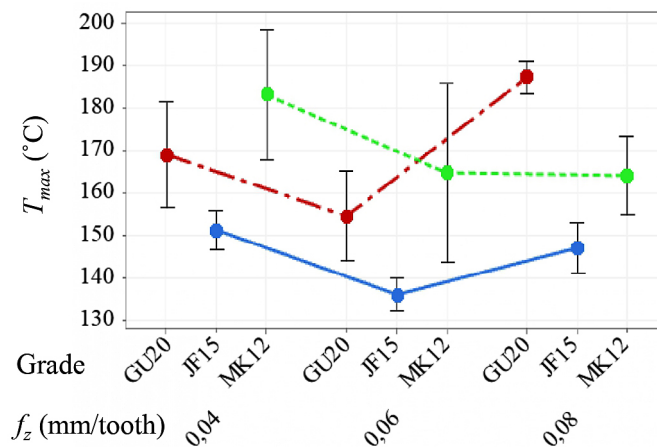


Figure 10. Maximum cutting zone temperature T_{max} vs. tool grade and feed f_z

size (JF15). For remaining carbides, the temperature values were higher by 10÷25% in comparison with JF15 and were maintained at a similar level. In case of MK12 (grain size 0.18 μm), the increased temperature in comparison with JF15 is a result of significantly smaller grains. The grain size defines, in the microscale, the tool-workpiece contact area. The smaller the grain, the larger the contact area and hence the larger the friction and the amount of generated heat. In case of GU20, a similar effect is a result of a higher cobalt content which reduces the thermal conductivity of the carbide and consequently, despite the similar grain size, causes a longer and more local temperature concentrations on the friction edge between the tool and the machined material. Such interpretation of results is in line with more general publications [38, 39]. The impact of feed on the cutting zone temperature is not significant.

In all tested cases, the results indicate a relationship between the feed and roughness parameters Ra and Rz . In general, the greater the feed, the higher the values of these parameters. The largest roughness was obtained for JF15 with the largest grain size. This effect can be attributed to two causes. Firstly, the smaller grain means a sharper cutting edge and, as already mentioned, a larger contact area between the tool and the workpiece. Secondly, as it has been proved, the reduced grain size leads to greater cutting forces and so to increased contact pressures. As a result, the plastic strained surface layer of the material has a lower roughness.

The cutting forces highly depend on the feed value and grow as the feed increases. The radial force values (F_y) were on average by 40% lower than the thrust force (F_x). The least cutting forces were obtained for JF15, and the greatest for MK12. The differences ranged from about 8% for feed $f_z=0.08$ mm/tooth to about 22% for $f_z=0.04$ mm/tooth and were similar for both cutting forces.

Impact of grain size on cutting tool wear

Figure 11 presents the relationship between the tool wear VB and the cutting time for various carbide grades. All tools were analysed until their wear reached $VB=0.2$ mm. In relation to the tests performed, each tool performed the planned test three times and the cutting edge wear referred to the average of the four cutting edges tested over the length of contact with the machined material. Figure 12 shows exemplary views of edge wear. The tool life was relatively long in case of MK12 and JF15 as it was 183 and 135 minutes, respectively.

A common tool wear curve can be divided into three stages, called an initial wear stage, a normal wear stage and a severe wear stage [40]. In case of the MK12 tool, these stages lasted from 0 to 15 minutes, from 15 to 160 minutes and from 160 to 183 minutes. The wear of the JF15 tool from the very beginning was uniformly linear until the critical point (~130 minutes), after which the wear progressed very fast and the critical value was reached within the next 5 minutes. No initial wear stage was observed in this case which proves a very quick wear of the surface structures of the tool. The probable reason of this phenomenon is a greater unevenness of the cutting edge whose protruding parts wear quickly and as a result the tool reaches the stabilized work condition earlier. However, a normal wear stage defining the duration of the effective tool work is the longest for the tool with the smallest grain size. In case of GU20, the tool life was only 15 minutes. The possible reason is its non-homogeneous structure which weakens the cutting edge. In addition, the increased amount of cobalt matrix in comparison with other tools reduces the tool hardness, consequently increasing its susceptibility to adhesive wear.

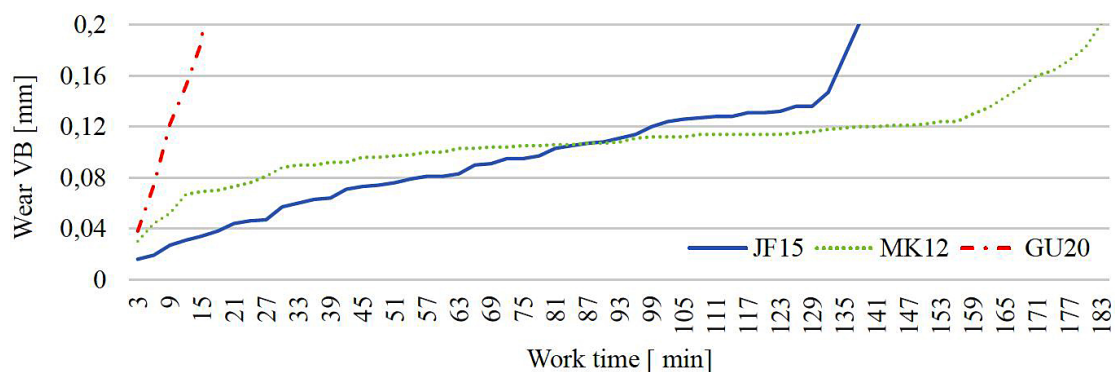


Figure 11. Tool wear VB vs. cutting time for various carbide grades

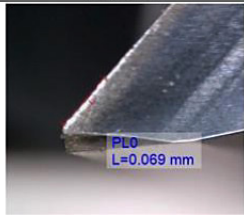
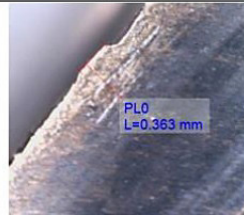
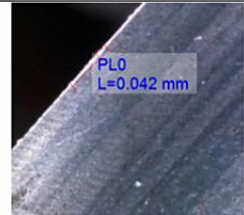
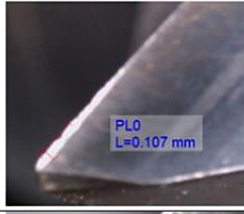
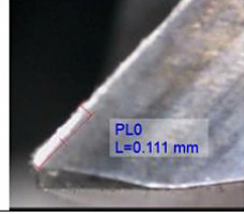
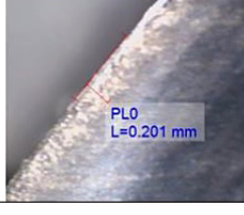
Time [min]	MK12	GU20	JF15
20			
87		tool worn out earlier	
183		tool worn out earlier	tool worn out earlier

Figure 12. Exemplary views of cutting edge wear

CONCLUSIONS

The studies involved side milling of a cuboidal block made of the AISI 316L steel. The machining was conducted with the use of proprietary tools made of the WC-Co carbide of various grades, covered with the AlCrN-based coating. The authors studied the impact of the tool material grade on the maximum cutting temperature, cutting forces, surface finish of the machined surface and the tool life. The analysis of the obtained results indicates that:

1. The studies have proved that the MK12 carbide with the 0.18 μm grain size is the optimal choice for machining of the 316L stainless steel. This tool had the longest life and allowed obtaining the lowest surface roughness parameters. Although the cutting zone temperature was highest in this case, it did not exceed 200°C and hence did not affect the properties of the machined surface significantly.
2. The GU20 carbide had the least durability. Its grain size was 0.28 μm and the cobalt content was the highest among all tools. The tool life was less than 15 minutes. The microscopic analysis indicates that this carbide has the most non-homogeneous structure which, in combination with the increased amount of matrix, considerably weakens the tool. Despite the lowest roughness values, it is hard to recommend

this carbide for machining of stainless steels in the conditions of the study.

3. The JF15 carbide gave the least cutting forces and the lowest temperature in the cutting zone. However, it should be noted that the differences in the obtained results were not significant (from 10 to 40 %, depending on the parameter and the carbide type). On the other hand, the surface quality was the poorest in this case. The values of R_a and R_z parameters were two/three times higher than in case of the remaining tools. The life of the JF15 tool was shorter by 25% than of the milling cutter made of MK12.
4. The feed values did not have a significant impact on the temperatures in the cutting zone, however strongly affected the forces. In each case, a twofold increase of the feed caused the F_x force to increase by 40 to 50% and the F_y force to increase even by 60%. This trend was similar for all tools.
5. The surface roughness parameters also increased when the feed increased. Depending on the tool material, the change of f_z from 0.04 to 0.08 mm/tooth makes the R_a increase twofold.

The findings presented in this article provide practical recommendations for improving the process of machining stainless steels using tools made of sintered carbide.

Acknowledgements

The authors extend their gratitude for assistance with the experimental studies to Poltra sp. z o.o. and to Mr. Łukasz Gajos for his technical support.

REFERENCES

1. Kaladhar M., Venkata Subbaiah K., Srinivasa Rao C.H. Machining of austenitic stainless steels – A review. *International Journal of Machining and Machinability of Materials* (2012) 12: 178–192.
2. Fernández-Abia A.I., García J.B., López De Lacalle L.N. High-performance machining of austenitic stainless steels. In: Davim J. Paulo (ed) *Machining and machine-tools*. Woodhead Publishing, (2013) 29–90.
3. Kumar A., Sharma R., Kumar S., Verma P. A review on machining performance of AISI 304 steel. *Mater Today Proc* (2022). <https://doi.org/10.1016/j.matpr.2021.11.003>
4. Song R.B., Xiang J.Y., Hou D.P. Characteristics of mechanical properties and microstructure for 316L austenitic stainless steel. *Journal of Iron and Steel Research International* (2011). [https://doi.org/10.1016/S1006-706X\(11\)60117-9](https://doi.org/10.1016/S1006-706X(11)60117-9)
5. Philip A.M., Chakraborty K. Some studies on the machining behaviour of 316L austenitic stainless steel. *Mater Today Proc* (2022). <https://doi.org/10.1016/j.matpr.2022.01.132>
6. Uysal A., Caudill J.R., Schoop J., Jawahir I.S. Minimising carbon emissions and machining costs with improved human health in sustainable machining of austenitic stainless steel through multi-objective optimisation. *International Journal of Sustainable Manufacturing* (2020). <https://doi.org/10.1504/IJSM.2020.107154>
7. Su Y., Zhao G., Zhao Y., Meng J., Li C. Multi-objective optimization of cutting parameters in turning AISI 304 austenitic stainless steel. *Metals (Basel)* (2020). <https://doi.org/10.3390/met10020217>
8. Du F., He L., Huang H., Zhou T., Wu J. Analysis and multi-objective optimization for reducing energy consumption and improving surface quality during dry machining of 304 stainless steel. *Materials* (2020) 13: 1–26.
9. Maurel-Pantel A., Fontaine M., Michel G., Thibaud S., Gelin J.C. Experimental investigations from conventional to high speed milling on a 304-L stainless steel. *International Journal of Advanced Manufacturing Technology* (2013) 69: 2191–2213.
10. Liu G., Zou B., Huang C., Wang X., Wang J., Liu Z. Tool damage and its effect on the machined surface roughness in high-speed face milling the 17-4PH stainless steel. *International Journal of Advanced Manufacturing Technology* (2016) 83: 257–264.
11. Ciftci I. Machining of austenitic stainless steels using CVD multi-layer coated cemented carbide tools. *Tribol Int* (2006) 39: 565–569.
12. Liu G.J., Zhou Z.C., Qian X., Pang W.H., Li G.H., Tan G.Y. Wear Mechanism of Cemented Carbide Tool in High Speed Milling of Stainless Steel. *Chinese Journal of Mechanical Engineering (English Edition)* (2018). <https://doi.org/10.1186/s10033-018-0298-2>
13. Alabdullah M., Polishetty A., Littlefair G. Impacts of Wear and Geometry Response of the Cutting Tool on Machinability of Super Austenitic Stainless Steel. *International Journal of Manufacturing Engineering*, 2016: 1–9.
14. Jianxin D., Jiantou Z., Hui Z., Pei Y. Wear mechanisms of cemented carbide tools in dry cutting of precipitation hardening semi-austenitic stainless steels. *Wear* (2011) 270: 520–527.
15. Martinho R.P., Silva F.J.G., Martins C., Lopes H. Comparative study of PVD and CVD cutting tools performance in milling of duplex stainless steel. *International Journal of Advanced Manufacturing Technology* (2019) 102: 2423–2439.
16. Nur R., Noordin M.Y., Izman S., Kurniawan D. Machining parameters effect in dry turning of AISI 316L stainless steel using coated carbide tools. *Proceedings of the Institution of Mechanical Engineers, Part E: Journal of Process Mechanical Engineering* (2017). <https://doi.org/10.1177/0954408915624861>
17. Sultan A.Z., Sharif S., Kurniawan D. Effect of Machining Parameters on Tool Wear and Hole Quality of AISI 316L Stainless Steel in Conventional Drilling. *Procedia Manuf* (2015) 2: 202–207.
18. Bembenek M., Dzienniak D., Dzindziora A., Sułowski M., Ropyak L. Investigation of the Impact of Selected Face Milling Parameters on the Roughness of the Machined Surface for 1.4301 Steel. *Advances in Science and Technology Research Journal* (2023). <https://doi.org/10.12913/22998624/170422>
19. Leppert T. (2012) Surface layer properties of AISI 316L steel when turning under dry and with minimum quantity lubrication conditions. *Proc Inst Mech Eng B J Eng Manuf*. <https://doi.org/10.1177/0954405411429894>
20. Szczołkarz N., Mrugalski R., Maruda R.W., Królczyk G.M., Legutko S., Leksycki K., Dębowski D., Pruncu C.I. Cutting tool wear in turning 316L stainless steel in the conditions of minimized lubrication (2021). *Tribol Int*. <https://doi.org/10.1016/j.triboint.2020.106813>
21. Natesh C.P., Shashidhara Y.M., Amarendra H.J., Shetty R., Harisha S.R., Shenoy P.V., Nayak M., Hegde A., Shetty D., Umesh U. Tribological and Morphological Study of AISI 316L Stainless Steel during Turning under Different Lubrication

- Conditions. *Lubricants* (2023). <https://doi.org/10.3390/lubricants11020052>
22. Inspektor A., Salvador P.A. Architecture of PVD coatings for metalcutting applications: A review. *Surf Coat Technol* (2014) 257: 138–153.
 23. Endrino J.L., Fox-Rabinovich G.S., Gey C. Hard AlTiN, AlCrN PVD coatings for machining of austenitic stainless steel. *Surf Coat Technol* (2006) 200: 6840–6845.
 24. Kulkarni A.P., Joshi G.G., Sargade V.G. Performance of PVD AlTiCrN coating during machining of austenitic stainless steel. *Surface Engineering* (2013) 29: 402–407.
 25. Bouzakis K.D., Tsouknidas A., Skordaris G., Bouzakis E., Makrimalakis S., Gerardis S., Katirtzoglou G. Optimization of wet or dry micro-blasting on PVD films by various Al₂O₃ grain sizes for improving the coated tools' cutting performance. *Tribology in Industry* (2011) 33: 49–56.
 26. Tillmann W., Stangier D., Hagen L., Schröder P., Krabiell M. Influence of the WC grain size on the properties of PVD/HVOF duplex coatings. *Surf Coat Technol* (2017) 328: 326–334.
 27. Petersson A., Ågren J. Constitutive behaviour of WC-Co materials with different grain size sintered under load. *Acta Mater* (2004) 52: 1847–1858.
 28. Wang H., Gee M., Qiu Q., Zhang H., Liu X., Nie H., Song X., Nie Z. Grain size effect on wear resistance of WC-Co cemented carbides under different tribological conditions. *J Mater Sci Technol* (2019). <https://doi.org/10.1016/j.jmst.2019.07.016>
 29. Saito H, Iwabuchi A, Shimizu T. Effects of Co content and WC grain size on wear of WC cemented carbide. *Wear* (2006) 261: 126–132.
 30. Bouzakis K.D., Michailidis N., Skordaris G., Tsouknidas A., Makrimalakis S., Bouzakis E. Grain size effect of pre- and post-coating treated cemented carbides on PVD films' adhesion and mechanical properties. *Materwiss Werksttech* (2013) 44: 697–703.
 31. Tang J., Xiong J., Guo Z., Yang T., Liang M., Yang W., Liu J., Zheng Q. Microstructure and properties of CVD coated on gradient cemented carbide with different WC grain size. *Int J Refract Metals Hard Mater* (2016). <https://doi.org/10.1016/j.ijrmhm.2016.09.003>
 32. Jian X.G., Chen M., Sun F.H., Ma Y.P., Zhang Z.M. Study on the effects of substrate grain size on diamond thin films deposited on tungsten carbide substrates. *Key Eng Mater.* (2004). <https://doi.org/10.4028/www.scientific.net/kem.274-276.1137>
 33. Polini R., Bravi F., Casadei F., D'Antonio P., Traversa E. Effect of substrate grain size and surface treatments on the cutting properties of diamond coated Co-cemented tungsten carbide tools. *Diam Relat Mater.* (2002) [https://doi.org/10.1016/S0925-9635\(02\)00020-1](https://doi.org/10.1016/S0925-9635(02)00020-1)
 34. Parihar R.S., Gangi Setti S., Sahu R.K. Effect of sintering parameters on microstructure and mechanical properties of self-lubricating functionally graded cemented tungsten carbide. *J Manuf Process* (2019) 45: 498–508.
 35. Ślusarczyk Ł., Franczyk E. Estimation of temperature in the cutting area during orthogonal turning of grade 2 titanium. *International Journal of Advanced Manufacturing Technology* (2023). <https://doi.org/10.1007/s00170-023-10877-5>
 36. Zhang Z., Liu Z., Ren X., Zhao J. Prediction of Tool Wear Rate and Tool Wear during Dry Orthogonal Cutting of Inconel 718. *Metals (Basel)* (2023) 13: 1225
 37. Zawada-Michalowska M., Pieśko P., Józwick J. Tribological aspects of cutting tool wear during the turning of stainless steels. *Materials* (2020). <https://doi.org/10.3390/ma13010123>
 38. Wang H., Webb T., Bitler J.W. Study of thermal expansion and thermal conductivity of cemented WC-Co composite. *Int J Refract Metals Hard Mater* (2015). <https://doi.org/10.1016/j.ijrmhm.2014.06.009>
 39. Vornberger A., Pötschke J., Gestrich T., Herrmann M., Michaelis A. Influence of microstructure on hardness and thermal conductivity of hardmetals. *Int J Refract Metals Hard Mater* (2020). <https://doi.org/10.1016/j.ijrmhm.2019.105170>
 40. Chuangwen X., Jianming D., Yuzhen C., Huaiyuan L., Zhicheng S., Jing X. The relationships between cutting parameters, tool wear, cutting force and vibration. *Advances in Mechanical Engineering* (2018). <https://doi.org/10.1177/1687814017750434>